Dendritic Molecular Transporters Provide Control of Delivery to Intracellular Compartments

Kui Huang,[†,§] Bryan Voss,[‡,§] Disha Kumar,[†] Heidi E. Hamm,*[,‡] and Eva Harth*[,†,‡]

Department of Chemistry, Vanderbilt University, 7619 Stevenson Center, Nashville, Tennessee 37235, and Department of Pharmacology, Vanderbilt University Medical Center, 442 Robinson Research Building, Nashville, Tennessee 37232-6600 .
Received September 13, 2006; Revised Manuscript Received November 16, 2006

Novel biocompatible macromolecular vectors were developed that not only enable transport of bioactive cargo across the cell membrane but also control the delivery into defined intracellular compartments. This work describes the synthesis and design of two non-peptidic fluorescently labeled Newkome-type dendrimers, differentiated over a varied alkyl spacer with guanidine end moieties. The internalization of the fluorescein-labeled molecular transporter into mammalian cells showed strong subcellular localizations, evident with both live cells and fixed cells costained with DAPI, a nuclear stain. We observed that the subcellular distribution of these vectors varied significantly, as one of the vectors concentrates in the nucleus (**FD-1**) while the other (**FD-2**) concentrates in the cytosol. All experiments performed with NIH-3T3 fibroblasts and human microvascular endothelial cells (HMEC) showed similar results. The differential localization patterns of the two molecular transporters can be controlled through the variation of alkyl spacer length at the terminal generation of the dendrimer. Intracellular delivery of bioactive entities into specific subcellular locations, utilizing this practical approach, might overcome limitations in drug delivery and pioneer future technologies in drug transport.

INTRODUCTION

The development of novel approaches that facilitate cellular uptake of a variety of physiologically and therapeutically active agents relies on the elucidation of new molecular transporter/translocator molecules and methodologies. In the past several years, strategies to overcome the limiting uptake of the plasma membrane have included cell-permeable peptide vectors (*1*−*4*), such as Tat peptide and other various arginine-rich oligopeptides (*5*−*9*). HIV−Tat peptide (R_{49}KKRRQRRR$_{57}$) and its arginine-rich derivatives have been given much attention, primarily due to their high efficiency, short sequence, and capabilities of transporting various types of molecular structures, such as small molecular weight compounds, oligonucleotides, magnetic beads, plasmid DNA, and even a full 129 kDa protein, across the membranes of most cell types (*10*−*16*). In particular, uptake assays of oligoarginines identified nona-arginines as being superior over traditional Tat peptides. The subcellular localization profile of synthetic oligoarginine peptides appeared to be in both the cytoplasm and nucleus, which is similar to that of HIV−Tat (49−57) (*7*, *13*, *17*−*19*). However, our goal is to develop novel therapeutic strategies to deliver drugs directly to intracellular sites such as the nucleus or the cytosol, in order to limit unwanted intracellular probe metabolism and transport and reduce nonspecific effects, toxicity and dosage levels. Alternative delivery tools for drug delivery, gene therapy, and vaccine delivery are in high demand to overcome current limitations.

One attempt to develop transport vectors has been the investigation of selected lysine−arginine-rich human-derived peptide vectors (*20*). It was found that these peptides, once inside the cell, enable accumulation of therapeutic molecules in the cytoplasm or nucleus, depending on the specific vector used. However, these peptide or peptoid-based molecular transporters are limited again by high cost, scalability, solubility, and stability.

We sought to exploit non-peptidic branched architectures based on the reported observation that branched-chain arginine peptides resulted in different patterns of cellular localization (*21*). Dendritic structures have been recognized to be ideal building blocks for biomedical applications because of their monodispersity, high loading capacity, large-scale production, and bioconjugation capability (*22*−*24*). Despite numerous reports about the importance of guanidinium groups in the peptidic backbone of oligoarginines, relatively few attempts have been made using guanidine groups in branched dendritic scaffolds (*25*, *26*). For example, a recent paper by Wender et al. (*26*) employs the use of triamine-based diamino acids to form a series of octa-arginine dendrimers that show differences in uptake efficiency related to the structural flexibility of the dendritic architecture. In contrast to this study, we directed our efforts to develop dendritic structures which mimic features of branched polyarginines but provide means to target and control intracellular delivery. We investigated intracellular distributions and the time course of uptake in vivo with two different mammalian cell lines using confocal microscopy.

We proposed that for a molecular transporter to possess the aforementioned features the constitution of the dendritic backbone had to be one of the most compact, highly branched, and biocompatible structures possible. Through mimicking a regular peptidic backbone, by the implementation of highly symmetric macromolecular peripheries, the critical presentation of the guanidino groups to the biological systems are controlled by the length of the alkyl spacer. We focused on these parameters for two main reasons. One, the length and flexibility of the spacer in dendritic transporter have thus far been connected with enhanced and rapid cellular uptake, and two, factors for

* To whom correspondance should be addressed: (E.H.) E-mail: eva.harth@vanderbilt.edu. Phone: 615-343-3405. Fax: 615-343-1234. (H.E.H.) E-mail: heidi.hamm@vanderbilt.edu. Phone: 615-343-3533. Fax: 615-343-1084.

† Vanderbilt University.

‡ Vanderbilt University Medical Center.

§ Both authors contributed equally to this work.

10.1021/bc060287a CCC: $37.00
Published on Web 02/07/2007

Scheme 1. Structures of FD-1 and FD-2

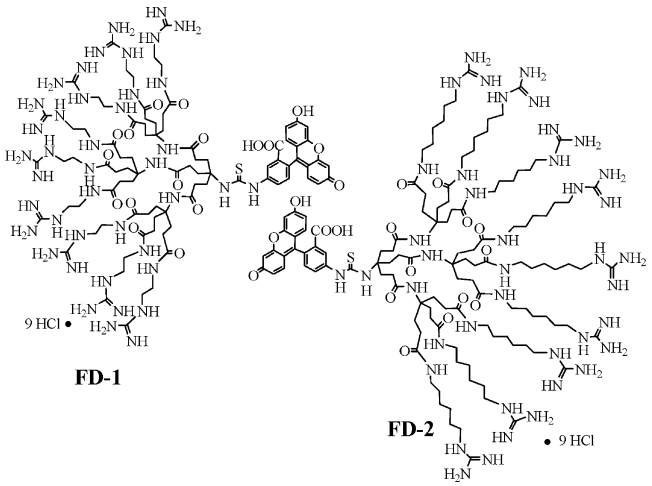

regulating intracellular specification have been unclear. Therefore, we sought to design and synthesize macromolecules with a differentiated flexible spacer to the guanidine functionality, but with a high-density arrangement on a symmetric and compact dendritic macromolecule.

In this study, we utilized the classic Newkome-type dendrimer as the structural building block, a compact yet highly branched structure in which the necessary nine end functionalities can be achieved in just one generation of dendritic growth (*11*, *27*). We report the design and synthesis of Newkome-type probe transporters, functionalized with guanidine end moieties and differentiated over a varied alkyl spacer to the scaffold, with a fluorophore conjugated to the focal point as the sample cargo molecule. We demonstrate the cell-penetrating capabilities of two new fluorescent macromolecular conjugates, FITC−dendrimer 1 (**FD-1**) and FITC−dendrimer 2 (**FD-2**), shown in Scheme 1. Interestingly, while these molecules feature similar, high levels of cellular uptake, they differ considerably in their subcellular localization (cytoplasm vs nucleus). There is a high potential for these molecular transporter molecules in both basic biomedical research and the clinical setting, as they could be used for the highly targeted delivery of a variety of bioactive molecules, thereby avoiding some of the common caveats of other drug delivery approaches, such as toxicity and limited cargo delivery (*16*).

EXPERIMENTAL PROCEDURES

Materials and Methods. All reagents and solvents were purchased from commercial sources and were used as received, unless otherwise stated. Spectra/Por Biotech cellulose ester and regenerated cellulose dialysis membranes were purchased from Spectrum Laboratories, Inc. Di-*tert*-butyl-4-[2-(*tert*-butoxycarbonyl)ethyl]-4-nitroheptanedicarboxylate **1** and 4-nitro-4-[2-(carboxyethyl)]heptanediacid **3** (Scheme 2) were prepared using a previously described method (*27*). Analytical TLC was carried out on Merck 250 μM silica gel 60 F_{254} plates, and spots were located by UV light or treatment with iodine. Column chromatography was conducted by silica gel (60−200 mesh) from Fisher Scientific. All NMR spectra were measured on a 400 MHz Bruker FT−NMR spectrometer. MALDI-MS were carried out on a Perspective Biosystems Voyager-DE STR (Framingham, MA) equipped with delayed extraction technology operating in linear mode (MALDI-MS data of known compounds not shown). 2′,4′,6′-Trihydroxyacetophenone (THAP) or 2,5-dihydroxybenzoic acid (DHBA) was used as the matrix with a matrix/analyte ratio of 1000:1. Reverse-phase high-performance liquid chromatography (RP-HPLC) was carried out with a Varian Prostar 210/215 HPLC using either an analytical column (Vydak, C18, 150 × 4.6 mm) or a preparative column (Alltec Alltima, C18, 250 × 22 mm). The products were eluted using a solvent gradient (solvent A = 0.05% TFA/H_2O; solvent B = 0.05% TFA/CH_3CN).

Synthesis of Di-*tert*-butyl-4-[2-(*tert*-butoxycarbonyl)ethyl]-4-aminoheptanedicarboxylate, "Behera's Amine" 2 (*27*). A solution of nitrotriester **1** (6.00 g, 0.0135 mol) in ethanol/dichloromethane (13:1, 140 mL) in a Parr hydrogenation bottle with 4 g of Raney-Nickel was stirred at 60 psi for 24 h at room temperature. The suspension was carefully filtered through Celite, and the removal of the solvent under reduced pressure gave the crude product. The residue was dissolved in dichloromethane (120 mL), and the resulting organic solution was washed sequentially with saturated $NaHCO_3$ (120 mL) and water (120 mL) and dried over anhydrous Na_2SO_4. The solvent was evaporated under reduced pressure to yield aminotriester **2** (5.2 g, 93%). ^{1}H NMR (400 MHz, $CDCl_3$): δ = 1.44 (s, CH_3, 27H), 1.95 (t, CH_2, 6H), 2.43 (t, CH_2, 6H). ^{13}C NMR (400 MHz, $CDCl_3$): δ = 27.98 (*C*H_3), 29.46 (*C*H_2CO), 31.47 (C*C*H_2), 56.99 (*C*NH_2), 80.96 (*C*CH_3), 172.30 (*C*O_2).

Synthesis of 9 Cascade:nitromethane [3]:(2-aza-3-oxopenylidyne):propionic acid 4 (*27*). To a solution of nitrotriacid **3** (0.65 g, 2.35 mmol) in dry THF (50 mL), 1-hydrobenzotriazole (HOBt) (0.96 g, 7.10 mmol), DCC (1.46 g, 7.10 mmol), and aminotriester **2** (3.54 g, 8.5 mmol) were added sequentially. The solution was stirred at room temperature for 40 h, then filtered and concentrated under reduced pressure. The crude product was purified by flash column chromatography, eluting with hexane/ethyl acetate (3:2) to yield the desired denron (3.00 g, 86%). ^{1}H NMR (400 MHz, $CDCl_3$): δ = 1.44 (m, CH_3, 81H), 1.95 (m, CH_2, 18H), 2.21 (m, CH_2, 30H), 6.20 (s, N*H*, 3H). ^{13}C NMR (400 MHz, $CDCl_3$): δ = 28.04, 29.74, 29.85, 31.28, 57.56, 80.69, 92.47, 170.46, 172.76. The dendron (1.47 g, 1 mmol) was stirred in 15 mL of formic acid overnight at room temperature. After the solvent was evaporated under reduced pressure, toluene was added and concentrated in vacuo to remove any residue of formic acid to give a white nona-acid **4** (0.95 g, 100%). ^{1}H NMR (400 MHz, DMSO): δ = 1.81 (m, CH_2, 18H), 2.11 (m, CH_2, 30H), 7.29 (s, N*H*, 3H), 12.10 (br, COO*H*). ^{13}C NMR (400 MHz, DMSO): δ = 28.03, 29.03, 30.08, 56.41, 93.31, 170.43, 174.42.

Synthesis of 9 Cascade:nitromethane [3]:(2-aza-3-oxopenylidyne):[propionic acid-(2-aminoethyl)amide] HCl Salt 5. To a solution of nona-acid **4** (2.12 g, 0.0022 mol) in DMF (30 mL), HOBt (2.68 g, 0.0198 mol) and DCC (4.09 g, 0.0198 mol) were added, and the solution was cooled to 0 °C. *N*-Boc-ethylenediamine (3.49 g, 0.0218 mol) in DMF (5 mL) was added dropwise, and the mixture was stirred for 48 h at room temperature, filtered, and concentrated under reduced pressure. The residue was dissolved in dichloromethane (100 mL), and the resulting organic solution was washed sequentially with 1 N HCl (100 mL), saturated $NaHCO_3$ (100 mL), and water (100 mL) and dried over anhydrous Na_2SO_4. The solvent was evaporated under reduced pressure, and the crude residue was purified by flash column chromatography eluting with 2% methanol in dichloromethane and gradually increasing to 10% methanol in dichloromethane to yield a white solid (2.5 g, 51%). ^{1}H NMR (400 MHz, CD_3OD): δ = 1.44 (m, CH_3, 81H), 1.80−2.10 (m, CH_2, 48H), 3.0−3.2 (m, CH_2, 36H), 6.20 (m, N*H*, 3H), 6.46 (m, N*H*, 8H), 7.71 (m, N*H*, 8H). ^{13}C NMR (400 MHz, CD_3OD): δ = 28.40, 31.24, 31.44, 31.80, 32.09, 40.66, 40.97, 59.14, 80.13, 94.42, 158.48, 173.48, 175.91. MALDI MS: calculated for $C_{103}H_{187}N_{22}O_{32}$ (M + Na^+), 2268.9; found, 2270.5. The resulting solid was dissolved in 1,4-dioxane (40 mL), the solution was cooled to 0 °C, and 4 M HCl in dioxane (40 mL) was added and stirred for 1 h at room temperature. Removal of the solvent under reduced pressure gave **5** as a white

Scheme 2. Synthetic Scheme for FITC−Dendrimer Conjugates

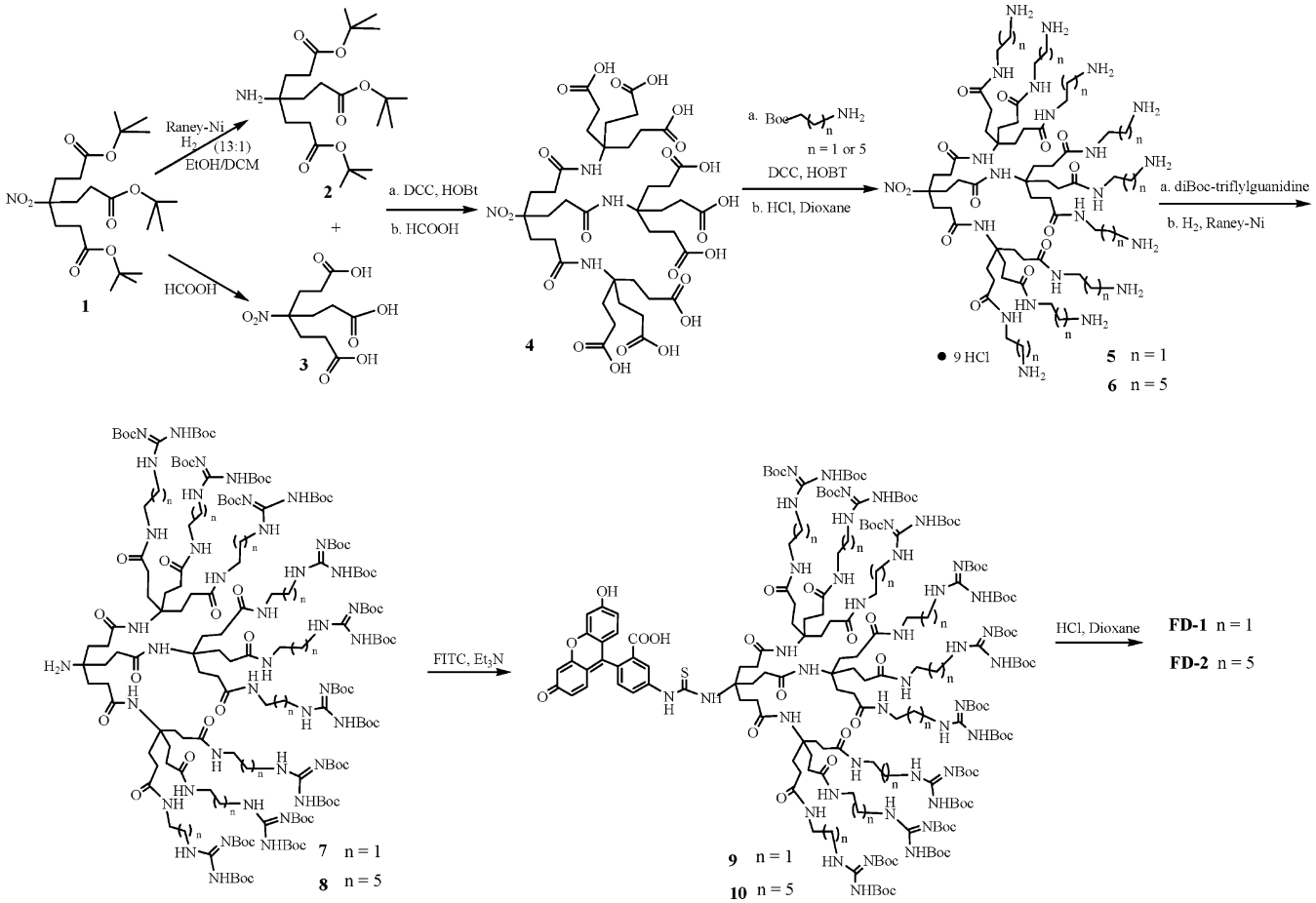

solid (1.86 g, 100%). ^{1}H NMR (400 MHz, D_2O/CD_3OD): δ = 1.70−2.15 (m, CH_2, 48H), 3.30 (m, CH_2, 18H), 3.36 (m, CH_2, 18H). ^{13}C NMR (400 MHz, D_2O/CD_3OD): δ = 27.61, 27.98, 28.86, 35.11, 37.41, 56.29, 92.01, 171.84, 174.98. MALDI MS: calculated for $C_{58}H_{124}Cl_9N_{22}O_{14}$ (M + H^+), 1673.9; found, 1674.8.

Synthesis of 9 Cascade:nitromethane [3]:(2-aza-3-oxopenylidyne):[propionic acid-(6-aminohexyl)amide] HCl Salt 6. To a solution of nona-acid **4** (1.2 g, 0.0012 mol) in DMF (20 mL), HOBt (1.514 g, 0.0112 mol) and DCC (2.311 g, 0.0112 mol) were added and the solution cooled to 0 °C. *N*-Boc-1,6-diaminohexane (2.66 g, 0.0123 mol) in DMF (5 mL) was added dropwise, and the mixture was stirred for 48 h at room temperature, filtered, and concentrated under reduced pressure to give the crude product. The residue was dissolved in dichloromethane (80 mL), and the solution was washed with 1 N HCl (80 mL), saturated $NaHCO_3$ (80 mL), and water (80 mL) and dried over anhydrous Na_2SO_4. The solution was concentrated under reduced pressure, and the crude product was purified by flash column chromatography eluting with 2% methanol in dichloromethane and gradually increasing to 10% methanol in dichloromethane to yield a white solid (1.68 g, 49%). ^{1}H NMR (400 MHz, CD_3OD): δ = 1.2−1.6 (m, CH_3, CH_2, 153H), 1.80−2.10 (m, CH_2, 48H), 3.0−3.2 (m, CH_2, 36H). ^{13}C NMR (400 MHz, CD_3OD): δ = 27.54, 28.85, 30.37, 30.90, 31.28, 31.60, 32.14, 40.58, 41.24, 59.13, 79.30, 94.30, 158.49, 173.50, 175.56. MALDI MS: calculated for $C_{139}H_{259}N_{22}O_{32}$ (M + H^+) 2750.7; found, 2784.03. The product was then dissolved in 1,4-dioxane (40 mL) and the solution cooled to 0 °C; 4 M HCl in dioxane (40 mL) was added and stirred for 1 h at room temperature. Removal of the solvent under reduced pressure gave **6** as a white solid (1.32 g, 100%). ^{1}H NMR (400 MHz, D_2O/CD_3OD): δ = 1.10−1.60 (m, CH_2, 72H), 1.7−2.2 (m, CH_2, 48H), 3.30 (m, CH_2, 18H), 3.36 (m, CH_2, 18H). ^{13}C NMR (400 MHz, D_2O/CD_3OD): δ = 26.89, 27.42, 28.21, 28.90, 35.03, 37.68, 56.28, 91.89, 172.3, 175.50. MALDI MS: calculated for $C_{94}H_{196}Cl_9N_{22}O_{14}$ (M + H^+), 2177.8; found, 2177.6.

Synthesis of 9 Cascade:nitromethane [3]:(2-aza-3-oxopenylidyne):propionic acid-(2-(1,3-bis-(*tert*-butoxycarboyl)guanidino)ethyl)amide 7. The resulting HCl salt of **5** (1.53 g, 0.92 mmol) was dissolved in methanol (80 mL), and the solution was cooled to 0 °C. Et_3N (3.5 mL) was added, followed by *N*,*N*′-diBoc-*N*′′-triflylguanidine (4.2 g, 10.73 mmol), and the mixture was stirred for 24 h at room temperature. After the solvent was evaporated under reduced pressure, the residue was dissolved in dichloromethane (100 mL), and the solution was washed with 1 N HCl (100 mL), water (100 mL), and dried over anhydrous Na_2SO_4. After removal of the solvent under reduced pressure, the crude product was purified by flash column chromatography starting with 2% methanol in dichloromethane and gradually increasing to 10% methanol in dichloromethane to yield a white solid (2.88 g, 90%). ^{1}H NMR (400 MHz, CD_3OD): δ = 1.45 (m, CH_3, 81H), 1.51 (m, CH_3, 81H), 1.90−2.25 (m, CH_2, 48H), 3.30−3.52 (m, CH_2, 36H). ^{13}C NMR (400 MHz, CD_3OD): δ = 28.37, 28.67, 31.32, 31.67, 32.06, 39.74, 41.24, 59.02, 80.23, 84.35, 94.31, 153.91, 157.737, 164.38, 173.33, 175.87. MALDI MS: calculated for $C_{157}H_{278}N_{40}O_{48}$ (M^+), 3524.1; found, 3573.4. The resulting white solid (0.352 g, 0.10 mmol) was dissolved in ethanol (40 mL) and transferred into a hydrogenation vessel containing Raney-Nickel catalyst (5 g), and the suspension was stirred at 65 psi for 48 h at room temperature. After filtration through Celite, the solvent was removed under reduced presssure to give a **7** as a white solid (0.28 g, 80%). ^{1}H NMR of **7** (400 MHz, CD_3OD): δ = 1.46 (m, CH_3, 81H), 1.51 (m, CH_3, 81H), 1.90−2.25 (m, CH_2, 48H), 3.30−3.55 (m, CH_2, 36H). ^{13}C NMR (400 MHz, CD_3OD): δ

= 28.37, 28.67, 31.40, 31.76, 39.76, 41.27, 54.0, 58.86, 80.32, 84.37, 153.97, 157.81, 164.4, 175.61, 176.02. MALDI MS: calculated for $C_{157}H_{278}N_{40}O_{48}$ ($M + H^+$), 3495.1; found, 3496.3.

Synthesis of 9 Cascade:nitromethane [3]:(2-aza-3-oxopenylidyne):propionic acid-(6-(1,3-bis-(*tert*-butoxycarboyl)guanidino)hexyl)amide 8. The resulting HCl salt **6** (0.838 g, 0.385 mmol) was dissolved in methanol (50 mL), and the solution was cooled to 0 °C. Et_3N (1.45 mL) was added, followed by *N*,*N*′-diBoc-*N*′′-triflylguanidine (1.765 g, 4.51 mmol), and the solution was stirred at room temperature for 24 h and the solvent evaporated under reduced pressure. The crude product was purified by flash column chromatography eluting with 2% methanol in dichloromethane and gradually increasing to 10% methanol in dichloromethane to give a white solid (1.40 g, 91%). ^{1}H NMR (400 MHz, CD_3OD): δ = 1.15−1.55 (m, 234H), 1.70−2.15 (m, C*H*$_2$, 48H), 3.29−3.30 (m, C*H*$_2$, 36H). ^{13}C NMR (400 MHz, CD_3OD): δ = 27.70, 27.62, 28.33, 28.67, 30.08, 30.33, 31.30, 31.60, 40.48, 40.62, 41.27, 54.5, 59.14, 80.25, 84.40, 154.22, 157.49, 164.53, 173.50, 175.53. MALDI MS: calculated for $C_{193}H_{349}N_{40}O_{50}$ ($M + H^+$), 4030.1; found, 4031.8. The white solid (0.40 g, 0.10 mmol) was dissolved in ethanol (40 mL) and transferred into a hydrogenation bottle containing Raney-Nickel catalyst (5 g), and the suspension was stirred at 65 psi for 72 h at room temperature. After filtration through Celite, the solution was evaporated to under reduced pressure to give a white solid **8** (0.32 g, 80%). ^{1}H NMR of **8** (400 MHz, CD_3OD): δ = 1.46 (m, C*H*$_3$, 81H), 1.51 (m, C*H*$_3$, 81H), 1.90−2.25 (m, C*H*$_2$, 48H), 3.30−3.55 (m, C*H*$_2$, 36H). ^{13}C NMR (400 MHz, CD_3OD): δ = 28.37, 28.67, 31.40, 31.76, 39.76, 41.27, 54.0, 58.86, 80.32, 84.37, 153.97, 157.81, 164.4, 175.61, 176.02. MALDI MS: calculated for $C_{193}H_{350}N_{40}O_{48}$ ($M + H^+$), 4000.1; found, 4007.8.

Synthesis of 9 Cascade:fluoresceinylmethane [3]:(2-aza-3-oxopenylidyne):propionic acid-(2-guanidino)ethyl)amide HCl Salt FD-1. Fluorescein isothiocyanate (FITC, 0.14 g, 0.36 mmol) in DMF (1 mL) was added to a 1:1 mixture of DMF/dichloromethane (10 mL) containing dendron **7** (0.23 g, 0.066 mmol). The mixture was cooled to 0 °C, Et_3N (0.092 mL, 0.66 mmol) was added, and the solution was stirred overnight at room temperature. After removal of the solvent under reduced pressure, the residue was dissolved in dichloromethane (15 mL), and the resulting solution was washed with 1 N HCl (15 mL) and water (15 mL) and dried over anhydrous Na_2SO_4. The solution was concentrated under reduced pressure to afford the yellow solid of 9 cascade:fluoresceinylmethane[3]:(2-aza-3-oxopenylidyne):propionic acid−(2-(1,3-bis-(*tert*-butoxycarboyl)-guanidino)ethyl)amide **9** (0.23 g, 91%). ^{1}H NMR (400 MHz, CD_3OD): δ = 1.46 (m, C*H*$_3$, 81H), 1.51 (m, C*H*$_3$, 81H), 1.90−2.25 (m, C*H*$_2$, 48H), 3.30−3.55 (m, C*H*$_2$, 36H), 6.52−6.72 (br, 4H), 7.15 (br, 1H), 7.5 (br, 2H), 7.72 (br, 1H), 8.4 (br, 1H). MALDI MS: calculated for $C_{179}H_{294}N_{41}O_{53}S$, ($M + H^+$), 3899.5; found, 3901.9. The resulting yellow solid (200 mg, 0.052 mmol) was dissolved in 1,4-dioxane (10 mL), and the solution was cooled to 0 °C. 4 M HCl in dioxane (10 mL) was added, and the mixture was stirred overnight at room temperature. After removal of the solvent under reduced pressure, the residue was dissolved in water, the insoluble precipitate was filtered off, and the filtrate was concentrated under reduced pressure. The crude product was purified by RP-HPLC using a solvent gradient (solvent A = 0.05% TFA/H_2O; solvent B = 0.05% TFA/CH_3CN) to give water-soluble **FD-1** (50 mg, 44%). Alternatively, the crude product could be purified by dialysis, as described for FD-2, to give a pure compound. ^{1}H NMR (400 MHz, D_2O): δ = 1.85−2.30 (m, C*H*$_2$, 48H), 3.10−3.30 (m, C*H*$_2$, 36H), 6.9 (br, 2H), 7.10−7.2 (m, 3H), 7.4 (s, 2H), 7.5 (br, 1H), 8.1 (s, 1H). MALDI MS: calculated for $C_{89}H_{157}Cl_9N_{41}O_{17}S$, ($M + H^+$), 2425.6; found, 2427.20.

Synthesis of 9 Cascade:fluoresceinylmethane [3]:(2-aza-3-oxopenylidyne):propionic acid-(6-guanidino)hexyl)amide HCl Salt FD-2. FITC (0.096 g, 0.2256 mmol) in DMF (1 mL) was added to 1:1 mixture of DMF/dichloromethane (10 mL) containing nona-(Boc-guanidinohexyl) dendron amine **8** (0.300 g, 0.075 mmol). The mixture was cooled to 0 °C, Et_3N (72 μL) was added, and the solution was stirred overnight at room temperature. After removal of the solvent under reduced pressure, the residue was dissolved in dichloromethane (15 mL), and the resulting solution was washed with 1 N HCl (15 mL) and water (15 mL) and dried over anhydrous Na_2SO_4. The solvent was evaporated at reduced pressure, and the crude product was dissolved in methanol and purified by dialysis against methanol with SpectraPor Biotech regenerated cellulose membranes (MWCO = 3500) for 24 h. Removal of the methanol in vacuo gave a yellow solid of 9 cascade:fluoresceinylmethane[3]:(2-aza-3-oxopenylidyne):propionic acid−(6-(1,3-bis-(*tert*-butoxycarboyl)guanidino)hexyl)amide **10** (290 mg, 88%). ^{1}H NMR (400 MHz, CD_3OD): δ = 1.20−1.7 (m, C*H*$_3$, C*H*$_2$, 234H), 1.89−2.30 (m, C*H*$_2$, 48H), 3.10−3.40 (m, C*H*$_2$, 36H), 6.52−6.72 (br, 4H), 7.15 (br, 1H), 7.5−7.72 (br, 3H), 8.1 (br, 1H). MALDI MS: calculated for $C_{215}H_{366}N_{41}O_{53}S$, ($M + H^+$), 4405.5; found, 4406.7. The resulting yellow solid (200 mg, 0.052 mmol) was dissolved in 1,4-dioxane (10 mL) and the solution cooled to 0 °C; 4 M HCl in dioxane (10 mL) was added and the solution stirred overnight at room temperature. The precipitate was filtered off and dried to give the crude product. The solid was redissolved in water, insoluble precipitate was filtered off, and the filtrate was dialyzed against water with SpectraPor Biotech cellulose ester membranes (MWCO = 1000) for 48 h and lyophilized to yield water-soluble **FD-2** (127 mg, 96%). ^{1}H NMR (400 MHz, D_2O): δ = 1.1−1.50 (m, C*H*$_2$, 72H), 1.50−2.20 (m, C*H*$_2$, 48H), 3.10−3.30 (m, C*H*$_2$, 36H), 6.5−6.7 (br, 6H), 7.10 (m, 1H), 7.5 (br, 3H). MALDI MS: calculated for $C_{124}H_{226}Cl_9N_{41}O_{17}S$ (M^+), 2914.5; found, 2914.6.

Uptake Experiment Protocol. Fluorescent dendrimer uptake by mammalian cells was assessed using NIH-3T3 cells (American Type Culture Collection) and HMEC (human microvascular endothelial cells—Centers for Disease Control) grown on gelatin-coated coverslips and a Zeiss LSM 510 confocal microscope. NIH-3T3 cells were grown in DMEM (Invitrogen) supplemented with 10% FBS (Invitrogen), and HMEC were grown in MCDB-131 media (Mediatech) supplemented with 5% FBS (Invitrogen) and 2 mM L-glutamine (Invitrogen). A time course of fluorescent dendrimer entry into NIH-3T3 cells and HMEC was completed in triplicate as previously described for Tat peptides (*21*). Briefly, the cells were treated with the dendrimer molecules for the series of incubation times, washed three times with PBS, fixed with 3% paraformaldehyde at room temperature for 10 min, and analyzed using confocal microscopy. In order to confirm the data, these experiments were also completed without fixing the cells. These experiments were completed through the use of the VUMC Cell Imaging Resource (supported by CA68485 and DK20593).

DAPI Staining. NIH-3T3 cells grown on gelatin-coated coverslips were treated with **FD-1** (10 μM), **FD-2** (10 μM), or vehicle (water) for 60 min at 37 °C, washed, and fixed as previously described above (*21*). After the cells were permeabilized with 0.1% Triton X-100 and washed twice with PBS, they were incubated with 0.5 μg/mL of 4′,6-diamidino-2-phenylindole (DAPI—Invitrogen) for 30 min at room temperature in the dark. The coverslips were then washed twice with PBS and mounted. A Nikon fluorescent microscope with a UV filter was then used to image the samples.

TUNEL Assay. NIH-3T3 cells grown on gelatin-coated coverslips were treated with **FD-1** or **FD-2** (10 μM), vehicle (water), or 50% methanol (positive control for apoptosis) for

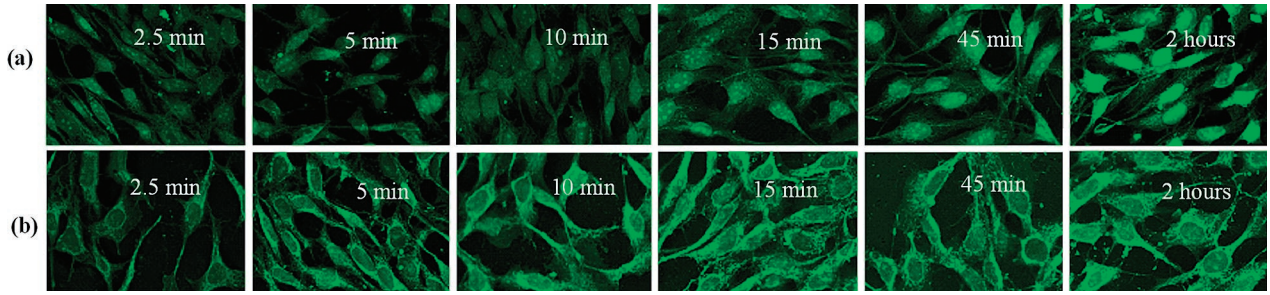

Figure 1. Time course of internalization of (a) **FD-1** and (b) **FD-2** into NIH-3T3 cells (fixed) at 37 °C. The conjugate concentration was 10 μM.

1 h at 37 °C and washed and fixed as previously described (*28*). An additional positive control involved the addition of DNAseI (New England BioLabs) to vehicle-treated cells that had been permeabilized with 0.1% Triton X-100 (Sigma). In order to label apoptotic nuclei, an in situ cell death detection kit with tetramethyl rhodamine (TMR-red) labeled dUTP (Roche Diagnostics) was used. The number of apoptotic nuclei in the **FD-1** and **FD-2** treated samples as compared to the positive and negative controls were measured with a Zeiss LSM-510 Confocal Microscope.

RESULTS AND DISCUSSION

In developing a new molecular transporter for targeted subcellular delivery of cargo molecules, we were drawn to the Newkome-type dendrimers, which are typically 1→3 C-branched polyamide macromolecules. These molecules are built from a "Behera's amine" monomer or its derivatives, that can be easily attached to a great variety of starting cores, surfaces, and polymers. Although the Newkome-type dendrimer is well-known, one of the drawbacks for a broader application is the elaborate synthesis of the monomer **2**. We efficiently synthesized the amine monomer **2** through improved hydrogenation of nitroester **1** and workup procedures of known literature methods (*27*). The synthesis of the dendron scaffold began with nitro-triacid monomer **3** reacting with "Behara's amine" monomer **2**, achieving the necessary nine end functionalities in only one generation of dendritic growth (Scheme 2). After the *t*-butyl groups were removed, the [G-1] nona-acid scaffold **4** was obtained in high yields. In order to introduce the guanidinium groups to the periphery of the dendrimer and provide diversity in the presentation of the guanidine groups to biological membranes, the carboxylic acid groups were first converted into Boc-protected amine groups. This was completed by reaction with a short alkyl linker (*N*-Boc-ethylendiamine) or a longer alkyl linker (*N*-Boc-1,6-diaminehexane), through established amide coupling reactions. After removal of the Boc groups, the nine free amines **5** or **6** were reacted with the guandinylating reagent (*29*) to give the guanidinylated dendritic scaffold in high yield (Scheme 2).

For preliminary uptake studies, a fluorescent probe was conjugated to the focal point of the molecular transporter, which served also as the test cargo molecule. The attachment of the fluorescein isothiocyanate (FITC) moiety to the guanidinylated scaffold started with a successful reduction of the nitro group at the focal point to an amino group via hydrogenation at room temperature in quantitative yields to form **7** or **8**. The free amino group was then directly reacted with FITC to form the Boc-protected FITC-labeled guanidino dendrimers **9** or **10**. After deprotection of the Boc-protected guanidine groups, FITC-labeled dendritic molecules were obtained and further purified by dialysis or HPLC, yielding pure **FD-1** and **FD-2**.

The two FITC−dendrimer conjugates were found to be highly water-soluble and were investigated for their capability to translocate through cell membranes. Internalization of **FD-1** and **FD-2** in mammalian cells was assessed using two different

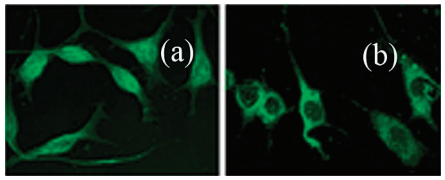

Figure 2. Confocal microscopy of (a) **FD-1** and (b) **FD-2** into unfixed NIH-3T3 cells at 37 °C. The conjugate concentration was 10 μM.

mammalian cell lines, NIH-3T3 fibroblasts and human microvascular endothelial cells (HMEC). Figure 1 shows the time course of uptake of **FD-1** and **FD-2** into NIH-3T3 fibroblasts at 37 °C. In this time course, the cells were treated with **FD-1** or **FD-2** for the series of time points shown, then washed, fixed with paraformaldehyde, and analyzed using confocal microscopy. The fluorescence was clearly observed within the cells 2.5 min after the addition of conjugates to the medium, which is comparable to the uptake rate of Tat−peptide (*13*, *21*). Furthermore, the extent of internalization increased in an incubation time-dependent manner, and the fluorescence intensity of cells treated with **FD-2** was near saturation after 10 min. However, the fluorescence intensity of cells treated with **FD-1** did not approach saturation until longer time points (45 min to 2 h). Interestingly, **FD-1** and **FD-2** exhibited differential patterns of subcellular localization, as **FD-1** appeared to concentrate in the nucleus with punctuated patterns similar to that of HIV Tat peptide, whereas **FD-2** appeared to concentrate in the cytosol. These data suggest that guanidine-rich **FD-1** and **FD-2,** bearing dendritic backbones, are internalized into cells in a similar manner to Tat peptides, but the length of the spacer at the terminal generation of the dendrimer not only controls the uptake rate (*30*), it also regulates the subcellular localization of the molecule and its putative cargo. For instance, the uptake levels of **FD-2** appeared to be generally higher than those of **FD-1** after the same incubation time at the same concentration. Therefore, the dendrimer with a hexyl spacer seems to cross the cell membrane faster than the molecule with an ethyl chain. As pointed out before, **FD-1** with the short spacer appeared to be localized mainly in the nucleus, whereas **FD-2**, with its longer spacer, was observed to reside mainly in the cytosol.

Fixed cells are usually used for confocal microscopy to obtain clear images, but recent studies indicate that cell fixation might lead to the artifactual redistribution of highly charged peptides (*31*, *32*). For this reason, the intracellular localization of **FD-1** and **FD-2** were also assessed using unfixed NIH-3T3 fibroblasts. In these experiments, the cells were treated with **FD-1** or **FD-2**, washed, and analyzed using confocal microscopy. The confocal images (Figure 2) showed that the distribution pattern of the fluorescent conjugates was consistent with that seen in fixed cells: **FD-1** with the short spacer appeared to be highly concentrated in the nucleus; while **FD-2**, with its longer spacer, was observed mainly in the cytosol. These experimental results strengthen the hypothesis that the cellular localization of **FD-1** and **FD-2** by fibroblasts is dominated to a high extent by the

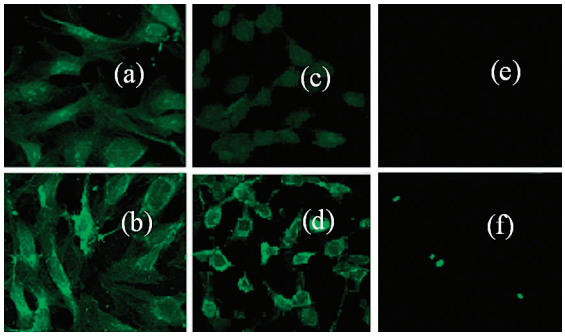

Figure 3. Confocal microscopy of human microvascular endothelial cells (HMEC) treated with (a) 10 μM of **FD-1** for 10 min at 37 °C; (b) 10 μM of **FD-2** for 10 min at 37 °C; (c) 10 μM of **FD-1** for 10 min at 4 °C; (d) 10 μM of **FD-2** for 10 min at 4 °C; (e) fluorescein isothiocyanate (FITC) for 1 h at 37 °C; (f) 10 μM of Boc-protected guanidinylated **FD-2** for 1 h.

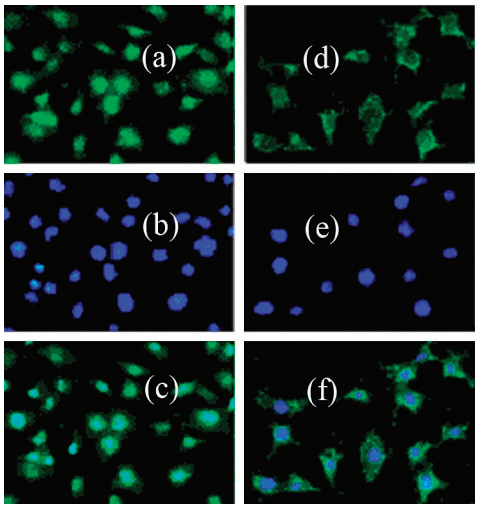

Figure 4. (a−f) NIH-3T3 cells were treated with **FD-1** (10 μM), **FD-2** (10 μM), or vehicle (water) for 60 min at 37 °C. Then, the cells were incubated with 0.5 μg/mL of 4′,6-diamidino-2-phenylindole (DAPI) for 30 min at room temperature in the dark.

length of the linker between the guanidine headgroups and the dendritic backbone. These results were confirmed with HMEC cells (Figure 3a,b).

The subcellular localization of **FD-1** and **FD-2** was further assessed by determining colocalization with the DAPI DNA stain. The 3T3 cells were treated with **FD-1** or **FD-2** and the nuclei were stained with DAPI, followed by the imaging of the cells with a fluorescent microscope equipped with a UV filter. **FD-1** colocalizes with DAPI (Figure 4a−c) to a much greater extent than **FD-2** (Figure 4d−f). These data provide solid evidence of the disparate subcelluar localization of the synthesized carriers, with **FD-1** concentrated mainly in the nucleus and **FD-2** concentrated in the cytosol.

In order to evaluate the effect of the guanidinium groups and the macromolecular dendritic structure on cellular uptake, control experiments were performed. HMEC were treated with free FITC and Boc-protected guanidinylated **FD-2**-dendrimer **10**. In the same time course of cellular uptake corresponding to the experiments of **FD-1** and **FD-2,** we observed extremely weak or no fluorescence for both compounds, as shown in Figure 3e,f. These observations suggest that the nanoscale hole formation mechanism (*33*), as previously proposed for the PAMAM dendrimer uptake mechanism, could be excluded and that the guanidino groups play a critical role in the cell permeability.

Additionally, we assessed the effect of temperature on the internalization of **FD-1** and **FD-2.** Figure 3c,d shows that the

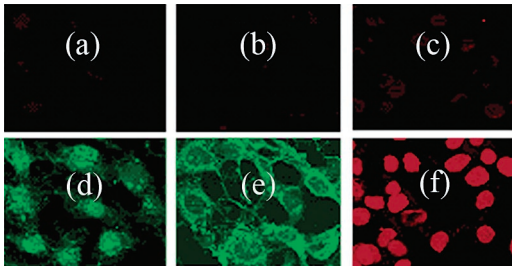

Figure 5. (a) **FD-1** + TMR − dUTP (red filter). (b) **FD-2** + TMR− dUTP (red filter). (c) Vehicle (water) + TMR − dUTP = negative control (red filter). (d) **FD-1** + TMR − dUTP (green filter). (e) **FD-2** + TMR − dUTP (green filter). (f) 50% Methanol + TMR− dUTP = positive control (red filter).

two conjugates are able to internalize into cells not only at 37 °C, but also at 4 °C, and no significant decrease in fluorescence intensity was observed. Although the exact translocation mechanism of guanidinylated peptides such as Tat and its derivatives remains controversial, these experiments suggest that active transport across the membrane is not needed and demonstrate that the internalization mechanism of the dendrimer carriers is similar to that of Tat and its derivatives.

The cytotoxicity of **FD-1** and **FD-2** was assessed using a well-characterized TUNEL assay and confocal microscopy to ensure the biocompatibility for further utilization. Neither **FD-1** nor **FD-2** caused 3T3 cell apoptosis in the dose range tested, with the highest dose being 10 μM for 60 min (Figure 5d,e), as only background staining of the nuclei (Figure 5a **FD-1**, red channel; Figure 5b, **FD-2**, red channel) similar to that of the negative control samples (Figure 5c) occurred. DNAse I (data not shown) and 50% methanol (Figure 5e) were used as the positive control treatments, as both cause nicks in the genomic DNA, and the nuclei of these cells were highly apoptotic as denoted by their strong staining pattern. Additionally, HMEC treated with 10 μM **FD-1** or **FD-2** for 60 min had no defect in intracellular calcium mobilization, as measured by the flex station, upon thrombin receptor stimulation when compared to HMEC treated with water (data not shown). These data suggest that **FD-1** and **FD-2**, at the experimental conditions tested, are not cytotoxic and are therefore ideal molecular carriers for the transport of putative bioactive cargo molecules.

CONCLUSION

In this report, we have described the synthesis of two novel dendritic molecular transporters, **FD-1** and **FD-2**, and investigated their uptake rate and intracellular distribution in mammalian cell lines using confocal microscopy. The design features of this macromolecule display a compact, biocompatible Newkome dendrimer scaffold with guanidine groups differentiated over an alkyl spacer. The combination of flexible spacer units conjugated to a highly symmetric dendritic backbone affords an increased density presentation of critical guanidine groups on the scaffold, without neglecting the necessity of structural flexibility for cellular uptake. We observed that the shorter alkyl spacer of **FD-1** directed the uptake of the transporter mainly into the nucleus, while **FD-2**, with the longer alkyl spacer, concentrated its fluorescent cargo in the cytosol. The critical role of the length of the hydrophobic alkyspacer, in this particular macromolecular design, has never been shown and allows for the directed subcellular delivery of bioactive cargo molecules utilizing scalable, biocompatible macromolecular carriers. Our results suggest that the synthetic approach of these molecular transporters and their unique targeting abilities will advance the development of novel vaccine vectors and drug delivery systems to overcome the limitations of current technologies.

ACKNOWLEDGMENT

We acknowledge gratefully Vanderbilt University for a junior faculty startup fund (E.H.) and the National Institutes of Health supporting this work (NIH EY06062, EY10291, HL84388) (H.H.). B.V. was supported by an American Heart Association pre-doctoral fellowship.

LITERATURE CITED

(1) Langel, Ü. (2002) *Cell-penetrating peptides: Processes and applications*. CRC Press, London.
(2) Lindsay, M. A. (2002) Peptide-mediated cell delivery: application in protein target validation. *Curr. Opin. Pharmacol. 2*, 587−594.
(3) Bennett, R. P., and Dalby, B. (2002) Protein delivery using VP22. *Nat. Biotechnol. 20*, 20−20.
(4) Derossi, D., Joliot, A. H., Chassaing, G., and Prochiantz, A. (1994) The 3rd helix of the antennapedia homeodomain translocates through biological-membranes. *J. Biol. Chem. 269*, 10444−10450.
(5) Joliot, A., and Prochiantz, A. (2004) Transduction peptides: from technology to physiology. *Nat. Cell Biol. 6*, 189−196.
(6) Fukati, S. (2006) Oligoargine vectors for intracellular delivery: design and cellular-uptake mechanisms. *Biopolymers 84*, 241−249.
(7) Rothbard, J. B., Jessop, T. C., and Wender, P. A. (2005) Adaptive translocation: the role of hydrogen bonding and membrane potential in the uptake of guanidinium-rich transporters into cells. *Adv. Drug Delivery Rev. 57*, 495−504.
(8) Brooks, H., Lebleu, B., and Vives, E. (2005) Tat peptide-mediated cellular delivery: back to basics. *Adv. Drug Delivery Rev. 57*, 559−577.
(9) Snyder, E. L., and Dowdy, S. F. (2004) Cell penetrating peptides in drug delivery. *Pharm. Res. 21*, 389−393.
(10) Wadia, J. S., Stan, R. V., and Dowdy, S. F. (2004) Transducible TAT-HA fusogenic peptide enhances escape of TAT-fusion proteins after lipid raft macropinocytosis. *Nat. Med. 10*, 310−315.
(11) Wender, P. A., Mitchell, D. J., Pattabiraman, K., Pelkey, E. T., Steinman, L., and Rothbard, J. B. (2000) The design, synthesis, and evaluation of molecules that enable or enhance cellular uptake: peptoid molecular transporters. *Proc. Natl. Acad. Sci. U.S.A. 97*, 13003−13008.
(12) Zhao, M., and Weissleder, R. (2004) Intracellular cargo delivery using tat peptide and derivatives. *Med. Res. Rev. 24*, 1−12.
(13) Vives, E., Brodin, P., and Lebleu, B. (1997) A truncated HIV-1 Tat protein basic domain rapidly translocates through the plasma membrane and accumulates in the cell nucleus. *J. Biol. Chem. 272*, 16010−16017.
(14) Fischer, P. M., Krausz, E., and Lane, D. P. (2001) Cellular delivery of impermeable effector molecules in the form of conjugates with peptides capable of mediating membrane translocation. *Bioconjugate Chem. 12*, 825−841.
(15) de la Fuente, J. M., and Berry, C. C. (2005) Tat peptide as an efficient molecule to translocate gold nanoparticles into the cell nucleus. *Bioconjugate Chem. 16*, 1176−1180.
(16) Torchilin, V. P., Levchenko, T. S., Rammohan, R., Volodina, N., Papahadjopoulos-Sternberg, B., and D'Souza, G. G. M. (2003) Cell transfection in vitro and in vivo with nontoxic TAT peptide-liposome-DNA complexes. *Proc. Natl. Acad. Sci. U.S.A. 100*, 1972−1977.
(17) Futaki, S., Suzuki, T., Ohashi, W., Yagami, T., Tanaka, S., Ueda, K., and Sugiura, Y. (2001) Arginine-rich peptides - An abundant source of membrane-permeable peptides having potential as carriers for intracellular protein delivery. *J. Biol. Chem. 276*, 5836−5840.
(18) Nori, A., Jensen, K. D., Tijerina, M., Kopeckova, P., and Kopecek, J. (2003) Tat-conjugated synthetic macromolecules facilitate cytoplasmic drug delivery to human ovarian carcinoma cells. *Bioconjugate Chem. 14*, 44−50.
(19) Torchilin, V. P. (2006) Recent approaches to intracellular delivery of drugs and DNA organelle targeting. *Annu. Rev. Biomed. Eng. 8*, 343−375.
(20) De Coupade, C., Fittipaldi, A., Chagnas, V., Michel, M., Carlier, S., Tasciott, E., Darmon, A., Ravel, D., Kearsey, J., Giacca, M., and Cailler, F. (2005) Novel human-derived cell-penetrating peptides for specific subcellular delivery of therapeutic biomolecules. *Biochem. J. 390*, 407−418.
(21) Futaki, S., Nakase, I., Suzuki, T., Youjun, Y., and Sugiura, Y. (2002) Translocation of branched-chain arginine peptides through cell membranes: flexibility in the spatial disposition of positive charges in membrane-permeable peptides. *Biochemistry 41*, 7925−7930.
(22) Gillies, E. R., and Frechet, J. M. J. (2005) Dendrimers and dendritic polymers in drug delivery. *Drug Discovery Today 10*, 35−43.
(23) Lee, C. C., MacKay, J. A., Frechet, J. M. J., and Szoka, F. C. (2005) Designing dendrimers for biological applications. *Nat. Biotechnol. 23*, 1517−1526.
(24) Tomalia, D. A., Naylor, A. M., and Goddard, W. A. (1990) Starburst dendrimers - molecular-level control of size, shape, surface-chemistry, topology, and flexibility from atoms to macroscopic matter. *Angew. Chem., Int. Ed. Engl. 29*, 138−175.
(25) Chung, H., Harms, G., Seong, C. M., Choi, B. H., Min, C., Taulane, J. P., and Goodman, M. (2004) Dendritic oligoguanidines as intracellular translocators. *Biopolymers 76*, 83−96.
(26) Wender, P. A., Kreider, E., Pelkey, E. T., Rothbard, J., and VanDeusen, C. L. (2005) Dendrimeric molecular transporters: synthesis and evaluation of tunable polyguanidino dendrimers that facilitate cellular uptake. *Org. Lett. 7*, 4815−4818.
(27) Newkome, G. R., Behera, R. K., Moorefield, C. N., and Baker, G. R. (1991) Cascade polymers: synthesis and characterization of one-directional arborols based on adamantane. *J. Org. Chem. 56*, 7162−7167.
(28) Nori, A., Jensen, K. D., Tijerina, M., Kopečcková, P., and Kopeček, J. (2003) Tat-conjugated synthetic macromolecules facilitate cytoplasmic drug delivery to human ovarian carcinoma cells. *Bioconjugate Chem. 14*, 44−50.
(29) Feichtinger, K., Sings, H. L., Baker, T. J., Matthews, K., and Goodman, M. (1998) Triurethane-protected guanidines and triflyldiurethane-protected guanidines: new reagents for guanidinylation reactions. *J. Org. Chem. 63*, 8432−8439.
(30) Wender, P. A., Kreider, E., Pelkey, E. T., Steinman, L., Rothbard, J. B., and VanDeusen, C. L. (2005) Dendritic molecular transporters: synthesis and evaluation of tunable polyguanidino dendrimers that facilitate cellular uptake. *Org. Lett. 7*, 4815−4818.
(31) Richard, J. P., Melikov, K., Vives, E., Ramos, C., Verbeure, B., Gait, M. J., Chernomordik, L. V., and Lebleu, B. (2003) Cell-penetrating peptides - a reevaluation of the mechanism of cellular uptake. *J. Biol. Chem. 278*, 585−590.
(32) Lundberg, M., and Johansson, M. (2002) Positively charged DNA-binding proteins cause apparent cell membrane translocation. *Biochem. Biophys. Res. Commun. 291*, 367−371.
(33) Hong, S. P., Bielinska, A. U., Mecke, A., Keszler, B., Beals, J. L., Shi, X. Y., Balogh, L., Orr, B. G., Baker, J. R., and Holl, M. M. B. (2004) Interaction of poly(amidoamine) dendrimers with supported lipid bilayers and cells: hole formation and the relation to transport. *Bioconjugate Chem. 15*, 774−782.

BC060287A